Delamination of thin film strips

Hong-hui Yu, John W. Hutchinson*

Division of Engineering and Applied Science, Harvard University, 29 Oxford Street, Cambridge, MA 02138, USA

Abstract

Delamination of residually stressed thin film strips is analyzed to expose the dependence on strip width and film/substrate elastic mismatch. Isotropic films and substrates are assumed. The residual stress in the film is tensile and assumed to originate from mismatch due to thermal expansion or epitaxial deposition. Full and partial delamination modes are explored. In full delamination, the interface crack extends across the entire width of the strip and releases all the elastic energy stored in the strip as the crack propagates along the interface. The energy release rate available to propagate the interface crack is a strong function of the strip width and the elastic modulus of the film relative to that of the substrate. The energy release rate associated with full delamination is determined as a function of the interface crack length from initiation to steady-state, revealing a progression of behavior depending in an essential way on the three dimensionality of the strip. The dependence of the energy release rate on the remaining ligament as the interface crack converges with the strip end has also been calculated, and the results provide an effective means for inferring interface toughness from crack arrest position. A partial delamination propagates along the strip leaving a narrow width of strip attached to the substrate. In this case, the entire elastic energy stored in the strip is not released because the strain component parallel to the strip is not relaxed. A special application is also considered, in which a residually stressed metal superlayer is deposited onto a polymer strip. The energy release rate for an interface crack propagating along the interface between the polymer and the substrate is determined in closed form.
© 2002 Elsevier Science B.V. All rights reserved.

1. Introduction

Thin film strips bonded to a substrate are commonly encountered in a variety of applications, such as metal conduction lines in microelectronic devices and optical waveguides in photonic devices. The film strips are often under residual stress, originating from epitaxy, deposition processes, or thermal expansion mismatch. Stress concentration at the film edges makes edges preferred sites to initiate delaminations along the film/substrate interface [1]. Examples of full delamination of film strips are shown in Fig. 1a, [2]. Partial delaminations are seen in Fig. 1b wherein the interface separation propagates along one side of the strip leaving a portion of the strip on the other side still bonded to the substrate. The mechanics underlying these two modes of delam-

ination will be studied with emphasis on the role of strip width and film/substrate elastic mismatch.

Attention is focussed on isotropic films strips of width w and thickness h with Young's modulus E_f, Possion's ratio ν_f and coefficient of thermal expansion α_f. The corresponding quantities for the isotropic substrate are E_s, ν_s and α_s. The substrate is assumed infinitely deep compared to the film thickness. For some of the results given in the paper, elastic mismatch is measured by the two Dundurs' parameters:

$$\alpha_D = \frac{E_f/(1-\nu_f^2) - E_s/(1-\nu_s^2)}{E_f/(1-\nu_f^2) + E_s/(1-\nu_s^2)} \quad \text{and}$$

$$\beta_D = \frac{1}{2}\frac{E_f(1+\nu_s)(1-2\nu_s) - E_s(1+\nu_f)(1-2\nu_f)}{E_f(1+\nu_s)(1-2\nu_s) + E_s(1+\nu_f)(1-2\nu_f)} \tag{1}$$

In most bi-material problems crack problems, the second Dundurs parameter, β_D, has relatively little influence on the energy release rate [3]. To reduce the number of parameters considered in this study, the role

*Corresponding author. Tel.: +1-617-495-2848; fax: +1-617-495-9837.

E-mail address: hutchinson@husm.harvard.edu (J.W. Hutchinson).
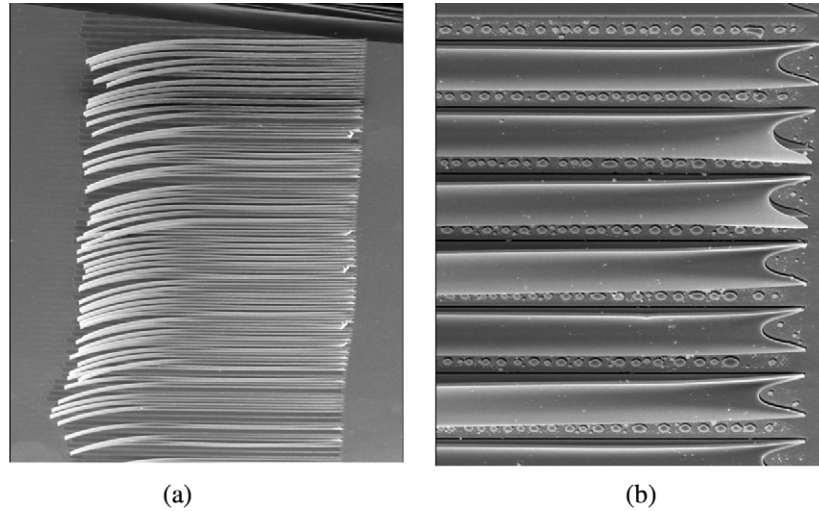
Fig. 1. Delamination of thin strips of an epoxy film with a superlayer of Ni under high residual tension from [2]. The interface which debonds lies between the epoxy and a self-assemble monolayer on a Au/Si substrate. (a) Full delamination; (b) partial delamination.

of β_D will be ignored by taking it to be zero in all the numerical calculations.

In this paper, the residual stress is assumed to originate from thermal expansion mismatch due to a temperature change, ΔT, from the zero-stress state. With $\Delta \alpha = \alpha_s - \alpha_f$ and $\Delta \alpha \Delta T > 0$, the residual stress in the bonded film is tensile, and this is the case that will be emphasized. Residual stress due to epitaxial mismatch can be recast in terms of thermal expansion mismatch.

If the width of the film strip is very large compared to the film thickness ($w/h \gg 1$), the stress state in the interior of the film (well away from the edges and the ends) is equi-biaxial tension with

$$\sigma_{xx} = \sigma_{yy} = \sigma_0 \equiv \frac{E_f \Delta \alpha \Delta T}{1 - \nu_f} \qquad (2)$$

At the other extreme for narrow strips when the width is comparable to the thickness ($w/h \approx 1$), the bonded film is constrained by the substrate in the x-direction but only minimally in the y-direction such that the stress state away from the ends is approximately uniaxial with

$$\sigma_{xx} = \sigma_0^* \equiv E_f \Delta \alpha \Delta T \qquad (3)$$

and $\sigma_{yy} \cong 0$, except near the film/substrate interface.

There are three fundamental elastic energy densities (strain energy per unit area) which are central to understanding the delamination of film strips. We denote them as Λ_B, Λ_0, Λ_U and term them, respectively, as the *energy density for biaxial stress*, *energy density under plane strain release*, and *energy density for uniaxial stress*. For a wide film strip, the elastic energy density in the bonded film away from the edges and ends, arising from the equi-biaxial stress state (Eq. (2)), is $(1 - \nu_f)\sigma_0^2 h / E_f$. This energy is relaxed in a zone along the edges and ends. For sufficiently wide and long

strips, the energy density in the interior region of the strip is

$$\Lambda_B = \frac{(1 - \nu_f)}{E_f} \sigma_0^2 h = \frac{E_f}{(1 - \nu_f)} (\Delta \alpha \Delta T)^2 h \qquad (4)$$

The steady-state energy release rate, $\bar{G}_{ss}$, for full delamination of a wide film strip will equal Λ_B, minus a deficit due to the edge zones. If the same wide film strip is released in such a way that it undergoes no strain change parallel to the crack front, then away from the sides the released energy density is

$$\Lambda_0 = \frac{(1 - \nu_f^2)}{2E_f} \sigma_0^2 h = \frac{(1 + \nu_f)E_f}{2(1 - \nu_f)} (\Delta \alpha \Delta T)^2 h \qquad (5)$$

This is usually referred to as the plane strain energy release rate, and under conditions when this constraint is applicable, the energy release is Λ_0. The elastic energy density stored in the narrow strip ($w/h \approx 1$) away from its ends under the uniaxial state (Eq. (3)) is $\sigma_0^{*2} h / (2E_f)$ such that

$$\Lambda_U = \frac{1}{2E_f} \sigma_0^{*2} h = \frac{1}{2} E_f (\Delta \alpha \Delta T)^2 h \qquad (6)$$

The steady-state energy release rate for full delamination of a narrow strip will be approximately Λ_U.

For positive values of ν_f, the fundamental energy densities are ordered according to $\Lambda_B > \Lambda_0 > \Lambda_U$. For $\nu_f = 1/3$, $\Lambda_0 / \Lambda_B = 2/3$ and $\Lambda_U / \Lambda_B = 1/3$. The importance of strip width and film/substrate elastic mismatch on delamination can be anticipated from the plot of $\bar{\Lambda}/\Lambda_B$ as a function of w/h in Fig. 2 for four values of elastic mismatch. Here, $\bar{\Lambda}$ is the energy density of an infinitely long strip averaged across the strip. The
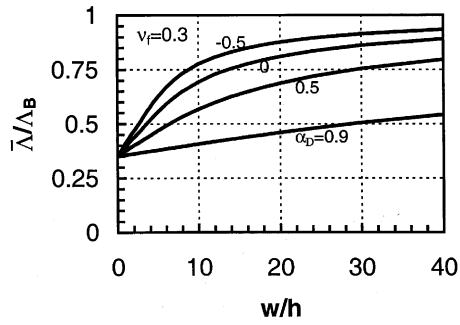
Fig. 2. Average energy density, $\bar{\Lambda}/\Lambda_B$, as a function of strip width to thickness ratio, w/h, for infinitely long strips for several values of the film/substrate elastic mismatch parameter, α_D. The steady-state energy release rate for full delamination of the strip equals the average energy density: $\bar{G}_{ss} = \bar{\Lambda}$.

method for computing $\bar{\Lambda}$ will be described in the next section, where it will also be noted that $\bar{G}_{ss}$ is $\bar{\Lambda}$ when full delamination occurs. The average energy density, $\bar{\Lambda}$, is well approximated by the uniaxial energy density, Λ_U, for $w/h < 2$. The approach of $\bar{\Lambda}$ to Λ_B as w/h increases depends strongly on the elastic mismatch. Even when there is no mismatch ($\alpha_D = 0$), however, $\bar{\Lambda}$ is only 85% of Λ_B when $w/h = 20$. If the substrate is very compliant compared to the film (e.g. $\alpha_D = 0.9$ in Fig. 2), $\bar{\Lambda}$ still remains only slightly above Λ_U when $w/h = 20$. These trends are consistent with the effective width of an edge zone as determined by [4], Fig. 4.8; [5]: it scales with $h(1 + [(1 - \nu_s^2)/(1 - \nu_f^2)]E_f/E_s)$. The implication of the trends in Fig. 2 is that the energy release rate available to drive a full delamination is highly dependent on strip width and elastic mismatch. The effect of thermal stress in uniformly spaced parallel strips on substrate curvature has been determined in related work [6].

2. Solution methods

2.1. Residual stress distribution and energy release rate for interface cracks

Fig. 3 provides a schematic for understanding how the residual stress in the film and substrate is distributed and a method by which it can be computed. Fig. 3a depicts the film bonded to the substrate and residually stressed due to the thermal mismatch, $\Delta\alpha\Delta T$. This distribution can be computed as the superposition of the two problems in Fig. 3b and c. In Fig. 3b, the substrate is unstressed with the film detached from the substrate and subject to a normal tension, σ_0, on all its edges. The film experiences the uniform, equi-biaxial stress state (Eq. (2)) that precisely accounts for the expansion or epitaxial mismatch, apart from redistribution around

the edges. In Fig. 3c, the film is bonded to the substrate and the sole loading is a normal compressive stress, σ_0, applied uniformly around the edges of the film (there are no residual stresses in this problem). This is called the reduced problem. The stresses associated with the reduced problem occur in both film and substrate and they are localized around the edges and ends of the film when the strip is wide and long. The full stress distribution (Fig. 3a) is the sum of the two distributions in Fig. 3b and c.

If a crack exists at the interface between the film and the substrate, it has no influence on the problem in Fig. 3b and, in particular, this problem makes no contribution to the stress intensity factors or energy release rate at any point along the crack edge. Thus, for any interface crack, the stress intensity factors and the energy release rate are obtained from the reduced problem in Fig. 3c in the presence of the crack. This decomposition is widely employed in plane problems. It is valid in 3D problems and greatly facilitates computations of some of the results presented below.

2.2. Steady-state energy release rates for full or partial delaminations

Fig. 4 illustrates the scheme for computing the average steady-state energy release rate of the interface delamination crack. Although the problem is 3D, the steady-state release rate can be computed from two 2D plane strain problems. Let $\bar{G}_{ss}$ be the steady-state energy release rate averaged across the propagating crack front (the forward front for the partial delamination in Fig.
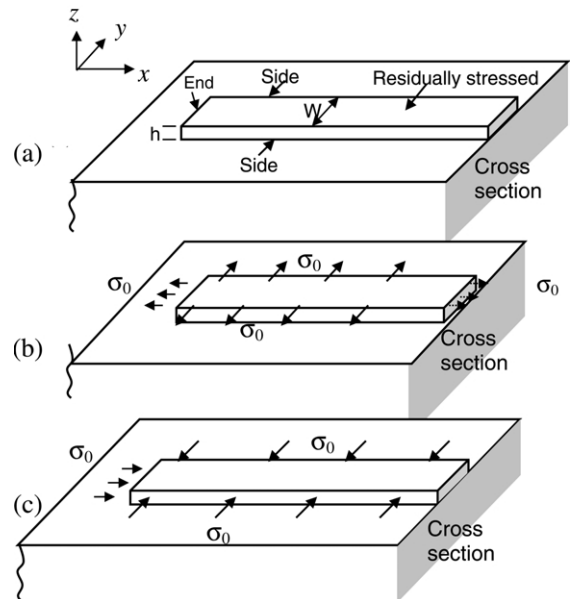

Fig. 3. (a) A residually stressed semi-infinite film strip on a substrate; (b) Detached strip subject to uniform pre-stress; (c) The reduced problem without initial residual stress.
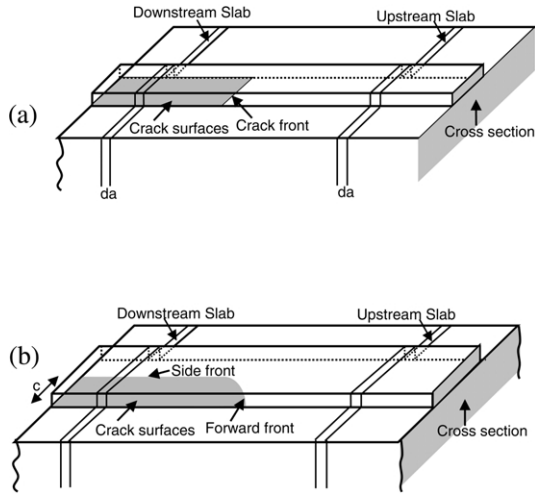
Fig. 4. Upstream and downstream sections for (a) steady-state full delamination and (b) steady-state partial delamination.

4b). Elementary energy accounting gives $\bar{G}_{ss}w = (SE_{upstream} - SE_{downstream})$, where $SE_{upstream} - SE_{downstream}$ is the difference between the strain energy per unit length of slab in the x-direction of slabs far ahead and far behind the crack front. The problem for each of these two slabs is 2D, and the result applies for a crack front of any shape.

For the *full delamination* in Fig. 4a, $SE_{upstream} = 0$ because both the film and the substrate are unstressed far downstream. The plane strain problem for the upstream slab gives

$$SE_{upstream} = \Lambda_B w + 2 \times \frac{1}{2} \int_0^h \sigma_0 u_y(z) dz \qquad (7)$$

where $u_y(z)$ is the displacement normal to the edge of the film in the reduced problem due to σ_0. The second contribution in Eq. (7) is negative and it represents the deficit in the stored energy due to relaxation along the strip edges. (The average energy density in the bonded strip introduced in Fig. 2 is $\bar{\Lambda} = SE_{upstream}/w$.) The contribution from the reduced plane strain problem in Eq. (7) has the general form

$$\left[(1 - \nu_f^2)\sigma_0^2 hw/E_f\right]g(\alpha_D, \beta_D, w/h)$$

and thus it follows that

$$\bar{G}_{ss} = \Lambda_B(1 - (1 + \nu_f)g(\alpha_D, \beta_D, w/h)) \qquad (8)$$

The function $(1 + \nu_f)g(\alpha_D, \beta_D, w/h)$, which accounts for the edge deficit in the release rate, is computed in a straightforward manner by applying a 2D finite element method to the reduced plane strain problem.

The energy release rate $\bar{G}_{ss}$ for the partial delamination in Fig. 4b can be computed in two ways: either by computing $SE_{downstream}$ directly using finite element method ($SE_{upstream}$ is identical to that just determined) or by the following alternative route. Consider the plane strain problem for the downstream geometry where an infinite interface crack parallel to the strip emerging from one side of the strip ($c = 0$) and spreading across the strip to length c with a bonded ligament of length $b = w - c$. Denote the energy release rate of this interface crack by G_{side}. It has the general functional form

$$G_{side} = \Lambda_0 f(\alpha_D, \beta_D, c/h, w/h) \qquad (9)$$

The function f is also computed using a 2D finite element code applied to the reduced problem. This energy release rate is of interest for two reasons. It controls the length of the remaining ligament of a partial delamination, as will be discussed later. It also provides the average steady-state energy release rate for the partial delamination front propagating down the strip according to

$$\bar{G}_{ss}c = \int_0^c G_{sides}(c)dc \qquad (10)$$

This result applies to a crack front of any shape. It follows from Eq. (9) that

$$\bar{G}_{ss} = \Lambda_0 \frac{h}{c} \int_0^{c/h} f\left(\alpha_D, \beta_D, \frac{c}{h}, \frac{w}{h}\right) d\left(\frac{c}{h}\right) \qquad (11)$$

2.3. Energy release rates requiring 3D calculations

The steady-state energy release rates of full and partial delaminations can be computed from 2D solutions as described above. Results for full delaminations for several non-steady state problems that are intrinsically 3D will also be presented. In these cases, the interface crack is taken to be straight and perpendicular to the sides of the strip. These problems have been solved using the finite element method with a 3D mesh [7]. The average energy release rate is computed by evaluating the J-integral as a function of position along the crack front and integrating to obtain the average value.

3. Steady-state energy release rates

3.1. Full delaminations

The effect of the width of the strip and the elastic mismatch between the film and the substrate, as measured by α_D, on the steady-state energy release rate of full delaminations is displayed in Fig. 2 by virtue of the fact that $\bar{G}_{ss} = \bar{\Lambda}$. For very narrow strips, $\bar{G}_{ss}$ approaches Λ_U, while for sufficiently large w/h, $\bar{G}_{ss}$ approaches Λ_B from below. For wide strips the relaxed edge zone along the sides has a fixed width which scales with the film thickness h and elastic mismatch according to $h(1 + [(1 - \nu_s^2)/(1 - \nu_f^2)]E_f/E_s)$ [4,7]. Thus, as the strip
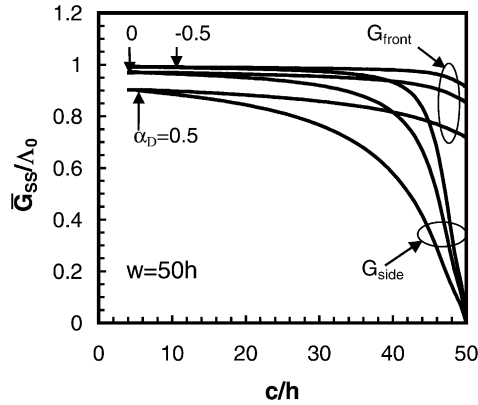
Fig. 5. Energy release rates for partial delamination as a function of delamination width c for $w/h = 50$. (a) Steady-state rate for the propagating front, $\bar{G}_{\text{front}}$; (b) Energy release rate along the side of the delamination crack well behind the front, G_{side}.

becomes wider the edge zones make smaller relative contributions to the average stored energy. The stiffer the substrate relative to the film, the narrower the edge zone, but it is never less than about one film thickness even in the limit when the substrate is infinitely stiff. As remarked in connection with the earlier discussion of Fig. 2, a system with $\alpha_D = -0.5$ (substrate modulus three times that of the film) or $\alpha_D = 0$ (no elastic mismatch) has $\bar{G}_{\text{ss}}$ approximately 15–10% below Λ_B when $w/h = 20$. By contrast, $\bar{G}_{\text{ss}}$ is only slightly above Λ_U and less than $\Lambda_B/2$ when $w/h = 20$ for a system with $\alpha_D = 0.9$, corresponding a film modulus approximately 20 times that of the substrate. In this case, the strip is effectively narrow as far as the energetics of delamination are concerned. Most metal or ceramic film strips on polymer substrates will have $\bar{G}_{\text{ss}} \cong \Lambda_U$ unless they are extremely wide.

3.2. Partial delaminations

Curves of G_{side} and $\bar{G}_{\text{ss}}$ as a function of delamination width, c/h, for the partial delamination are presented in Fig. 5 for a strip width $w/h = 50$ and several mismatches, α_D.

First, we direct attention to the energy release rate, G_{side}, on the straight crack front far behind the propagating front. If the strip were much wider than that shown (e.g. so wide that the edge zones have no interaction), one would observe that G_{side} rapidly rises to Λ_0 and then levels off at $c/h \approx 1/4$, as shown earlier for a semi-infinite film under plane strain interface cracking [8]. This is essentially what is seen in Fig. 5 for the case of the film with the smallest modulus relative to the substrate ($\alpha_D = -0.5$). (However, $c/h = 4$ is the smallest value for which G_{side} has been computed here.) Note that G_{side} will not exceed the plane

strain release density Λ_0. The extent to which G_{side} falls below Λ_0 in Fig. 5 for delaminations roughly halfway across the strip is due to the partial relaxation of stress across the entire strip because of its finite width, especially for a stiff film on a compliant substrate ($\alpha_D = 0.5$).

As $c \to w$, a phenomenon called a 'converging debond' [8,9] is observed with $G_{\text{side}} \to 0$. The effect is readily understood in terms of the relaxed energy stored in the remaining ligament in the edge zone. It is evident from the behavior displayed in Fig. 5 that the edge zone is on the order of $5h$ for a low film to substrate modulus ratio ($\alpha_D = -0.5$), increasing to roughly $20h$ for a high film/substrate modulus ratio ($\alpha_D = 0.5$). The edge zones are surprisingly large, consistent with the trends noted in connection with Fig. 2.

The steady-state energy release rate for the propagating partial delamination front, $\bar{G}_{\text{ss}}$, which is related to G_{side} by Eq. (11), is nearly independent of c/h with a slight drop as $c/h \to w/h$. It is also always below Λ_0, and one can show that for a partial delamination $\bar{G}_{\text{ss}}$ is always less than that for a full delamination, as expected on physical grounds due to the constraint provided by the attached ligament along one edge. It is for this reason that $\bar{G}_{\text{ss}}$ does not approach the corresponding result for the full delamination as $c \to w$.

3.3. Partial or full delamination?

For steady-state delamination, the energy release rate for full delamination always exceeds that for partial delamination, by a factor of $\Lambda_B/\Lambda_0 = 2/(1 + \nu_f)$ for sufficiently wide strips. Why then does full delamination (cf. Fig. 1a) not always take precedence over partial delamination (cf. Fig. 1b)? The question is a natural one based on the following. If the criterion $\bar{G}_{\text{ss}} = \Gamma_c$ is met for partial delamination, with Γ_c as the interface toughness (with units of energy/area), then clearly the full delamination energy release rate will exceed Γ_c.[1] Underlying the existence of partial delaminations is the converging debond effect as reflected by the behavior of G_{sides} as $c \to w$ in Fig. 5. Consider a delamination starting at a corner at one end of the strip and spreading down and across the strip (delaminations emerging from corner locations are considered in Ref. [10]). If the delamination is initiated in such a way that it extends in the length direction without reaching the far side of the strip, it may never be able to reach the strip edge. The energy release along that portion of the crack front diminishes sharply as the crack converges with edge.

---

[1] A possible effect of mode mix on interface toughness is not taken into account in this argument, but the difference between the mode mix for partial and full delaminations is not expected to be very large. The mode mix for the various interface crack geometries has not been computed in this study.
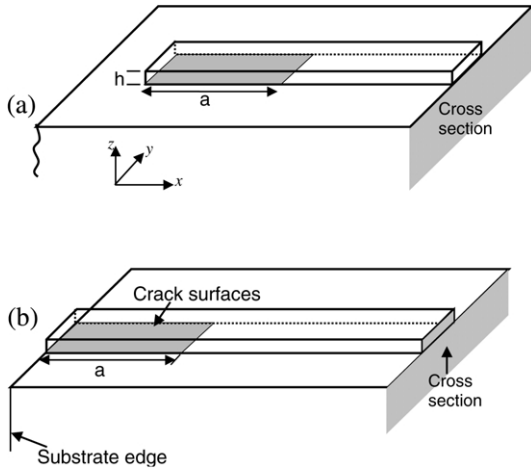
Fig. 6. Full delamination for two end geometries: (a) Strip end terminating in the interior of the substrate surface and (b) Strip end aligned with substrate edge.

On the other hand, if the delamination is initiated in such a way that the crack front extends across the entire strip, it can then propagate down the strip unimpeded as a full delamination. Strip delamination is one of many examples where the preferred fracture mode cannot be ascertained by energetic arguments alone. In the strip delaminations observed in the experiments [2] in Fig. 1, full delaminations were observed more often than partial delaminations, but starter cracks that extended across the entire strip were intentionally introduced at one end for most of these specimens. In general, partial delaminations are only to be expected if the strip width is sufficiently large such that $\bar{\Lambda}$ is well above Λ_U.

4. Strip/substrate geometry and crack length dependence

4.1. Influence of geometry at the end of the film strip on initiation of a full delamination

Consider the two geometries at the end of the strips shown in Fig. 6: one terminating on the interior of the substrate surface and the other with its end aligned with the edge of the substrate. Under plane strain conditions for infinitely wide strips, there is a significant difference between the two cases in the manner which the energy release rate approaches the steady-state limit [8]. For the strip terminating on the substrate interior, $\bar{G}$ approaches $\bar{G}_{ss}$ once the crack length is only a small fraction of the film thickness. By contrast, when the film end is aligned with the substrate edge, $\bar{G}$ remains well below $\bar{G}_{ss}$ for cracks that can be many times the film thickness, especially so if the film modulus is high compared to the substrate modulus. The extra compliance supplied by the edge of the substrate results in a

built-in protection against delamination initiation that does not exist for strips terminating on the substrate interior. This feature carries over to the strips of Fig. 6, with the additional complications associated with finite strip width.

The results of 3D finite element computations as described in Section 2.3 for the two strip end geometries are shown in Figs. 7 and 8. Fig. 7 reveals the influence of end geometry on an interface crack of length a extending from the end of a relatively narrow strip having $w/h = 2$. When the strip end is located on the substrate interior (Fig. 7a), $\bar{G}$ is very nearly its steady-state limit, $\bar{G}_{ss}$, when $a/h = 1/4$, the smallest crack lengths for which results have been computed. The steady-state asymptotes are denoted as dashed lines with dependence on elastic mismatch as discussed earlier. By contrast, for a narrow strip whose end is aligned with the edge of the substrate (Fig. 7b), a much longer crack is required to for $\bar{G}$ to approach the steady-state limit. If there is no elastic mismatch, $\bar{G}_{ss}$ is approached for $a/h \approx 5$, while if the film modulus is very large compared to that of the substrate ($\alpha_D = 9$), $\bar{G}$ is still well below steady-state limit when $a/h = 20$.
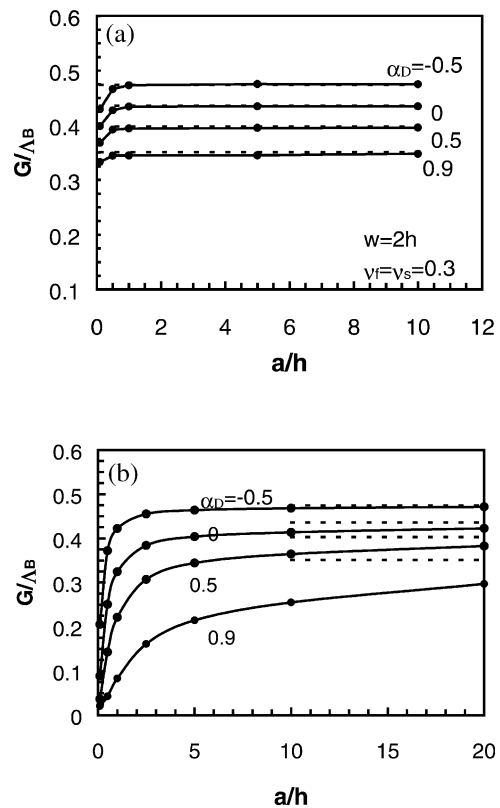

Fig. 7. Comparison of energy release rates, $\bar{G}$, for full delamination for a crack emerging from the end of a strip for an end terminating in the interior of the substrate (a) and for an end aligned with the substrate edge (b); in both cases for narrow strip with $w = 2h$.
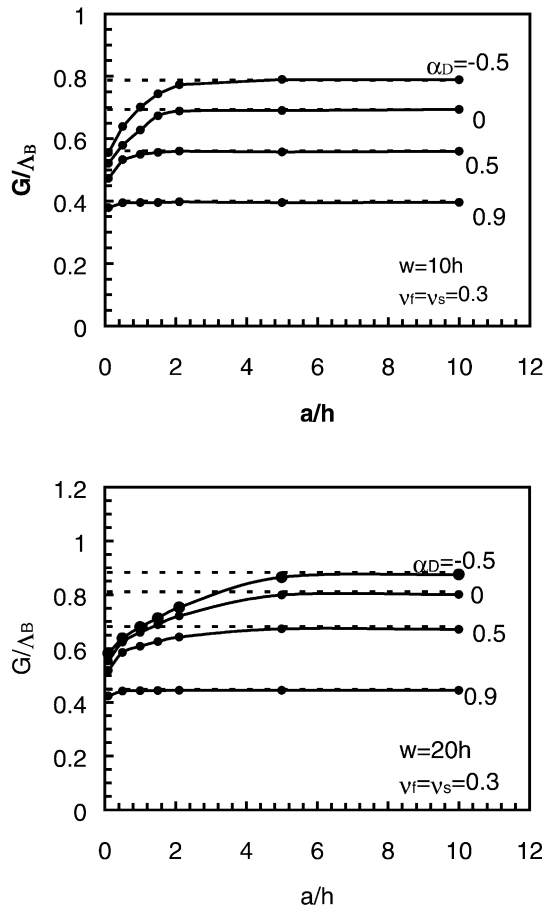
Fig. 8. Energy release rates, $\bar{G}$, for full delamination for cracks emerging from the end of a strips for an end terminating in the interior of the substrate for $w=10h$ and $w=20h$.

Further results for $\bar{G}(a)$ for wider strips whose ends are located on the substrate surface interior are presented in Fig. 8. As for the narrow strip, $\bar{G}$ jumps from 0 at $a/h=0$ to a relatively large intermediate value at $a/h=1/4$ (the smallest crack length for which calculations have been carried out here). Then, as a/h increases, $\bar{G}$ slowly increases approaching the steady-state limit (again shown as a dashed line) when $a \approx w/2$. When the crack is as long as, or longer than, $a \approx w/2$, essentially all the elastic energy stored in the separated portion of the strip well behind the tip is released and thus conditions for steady-state are met. For shorter cracks, when a is on the order of h, the separated portion of the strip is constrained in the direction parallel to the crack front. If the strip were even wider than those in Fig. 8, one would find that $\bar{G} \approx \Lambda_0$ for these intermediate crack lengths, but the values in Fig. 8 fall below Λ_0 due to the relative narrowness of these strips.

The full delamination behavior displayed in Figs. 7 and 8 is intrinsically 3D reflecting interactions among crack length, strip width and film/substrate elastic mis-

match. The steady-state energy release rate and its dependence on strip width and elastic mismatch is the key to understanding the behavior. Initiation of delamination depends on the behavior of short cracks on the order of the film thickness. Strips whose ends are aligned with the substrate edge have an inherent 'protection' against delamination initiation in the sense that fairly large initial flaws are needed to propagate a delamination. Much smaller flaws on the order of a fraction of the film thickness will initiate a delamination for a strip whose end terminates in the interior of the substrate.

4.2. Converging delaminations

Film width and elastic mismatch also influence the energy release rate of a delamination approaching the end of a strip or another delamination crack propagating the opposite direction (Fig. 9). This dependence is important because the distance of the arrest from the end of the strip or from the approaching delamination has been employed as a reliable experimental means of determining the interface toughness [2,11]. Plane strain behavior has been investigated in Refs. [8,9]. It was found that there is essentially no difference between the two cases considered in Fig. 9. For finite width strips, we expect that, as long as the bonded ligament of length b is greater than approximately $w/2$, there will be little difference between the two converging delamination situations depicted in Fig. 9. The computations carried out here have been limited to the symmetric case where two delaminations approach each other, as in Fig. 9b. The behavior is intrinsically 3D.

Average energy release rates, $\bar{G}(b)$, for full delaminations as a function of the remaining ligament, b, are shown in Fig. 10a for $w/h=2$ and in Fig. 10b for $w/h=20$. For sufficiently long ligaments, $\bar{G}=\bar{G}_{ss}$, where the steady-state release rate corresponds to the particular strip width and elastic mismatch (shown as dashed lines
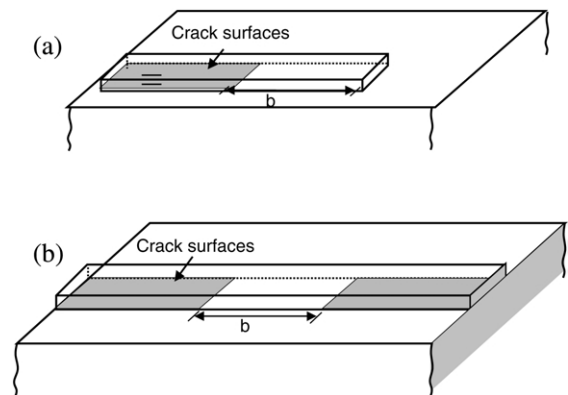

Fig. 9. Full delaminations converging on (a) a strip end and (b) on another delamination approaching from the opposite direction. The two configurations are quantitatively similar.
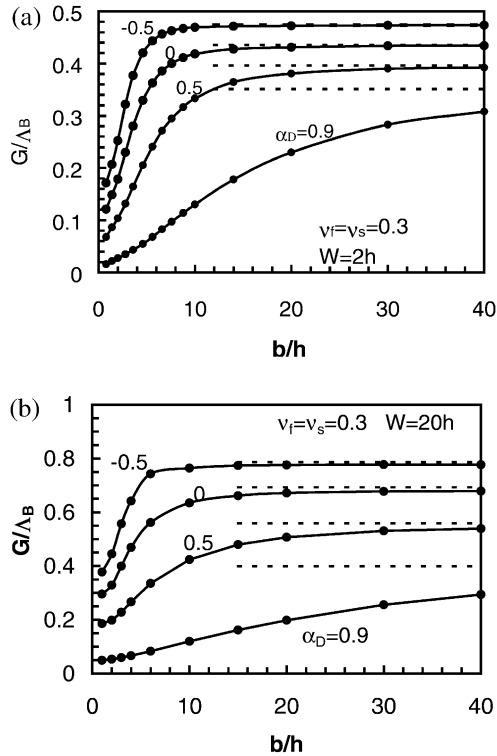
Fig. 10. Energy release rate as function of remaining ligament length for symmetric convergent debonding. (a) $w = 2h$; (b) $w = 20h$.

in Fig. 10). As the ligament length diminishes and the delamination senses its twin propagating in the opposite direction, $\bar{G}$ diminishes and approaches zero as $b \to 0$. The converging delaminations lower the stress in the attached portion of the film, leaving less stored elastic energy to be released. Delaminations sense each other at ligament lengths that are many times the film thickness, but depending in a surprisingly strong way on the strip width and elastic mismatch. Delaminations of films with high modulus relative to the substrate (e.g. $\alpha_D = 0.9$) sense each other at distances that can be many times the strip width when the strip is narrow. Even when there is no mismatch, the energy release rate of a narrow strip begins its gradual descent to zero at when the ligament is still several times the strip width. It is for this reason that the arrest location is a robust means of determining the critical $\bar{G}$ associated with interface toughness. The same behavior applies to the scenario in Fig. 9a with the delamination approaching the strip end. It is evident from the selected results in Fig. 10 that the energy release rate is a fairly strong function of the film width, elastic mismatch and remaining ligament. These dependencies must be known if the arrest location of a converging debond is to be used to ascertain interface toughness.

5. Superlayer on polymer film strip

The superlayer technique [12] to study the debonding of polymer–polymer interfaces whose chemistry was varied systematically [2]. In the experiments [2], a self-assembled monolayer (SAM) with either a CH_3 or a COOH end member, was placed on a Si substrate coated with a nano layer of Au. Then, an epoxy strip of thickness 1 μm was superposed. The toughness of the interface between the SAM and the epoxy was explored. While there is some residual tension in the epoxy, it is not nearly sufficient to supply the energy to drive the delamination crack. For this purpose, a top strip (the superlayer) of Ni is deposited by vapor deposition, bonding securely to the epoxy. The intrinsic residual tension due to deposition of the Ni is on the order of 1 GPa. The thickness of the Ni layer is increased until there is sufficient elastic energy stored in the Ni layer to drive the delamination. The elastic energy stored in the epoxy is negligible by comparison. The arrest location of the delamination was found to provide a more reliable means of determining the critical energy release rate associated with the interface toughness than the initiation value [2]. Almost inevitably, initiation is subject to uncertainty associated with the potency of initial flaws. Typically, the system is overstressed (or the superlayer overly thick) such that the steady-state energy release exceeds the interface toughness. Under these circumstances, the crack propagates dynamically and arrests in the converging debond region. If the relation between the energy release rate and the remaining ligament length of the strip is known, the SAM/epoxy interface toughness can be derived from measuring the ligament length. In the model presented below, for the purpose of calculating $\bar{G}$, the energy contributions from the SAM (which is only one molecular length in thickness) and from the epoxy are ignored. The epoxy contribution could readily be accounted for if it were of any consequence. For this calculation, the interface lies between the epoxy layer (E_1, ν_1) and the thick Si substrate (E_2, ν_2) (Fig. 11). The Ni layer (E_3, ν_3) on top has a residual tensile pre-stress, σ_0.
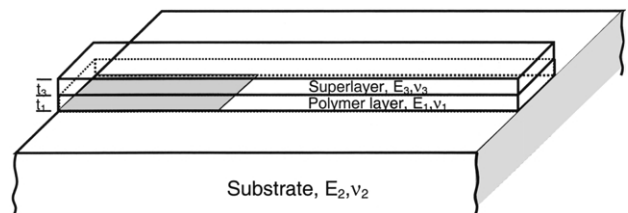

Fig. 11. Delamination of a bilayer. In the numerical example, the lower film is epoxy and the upper film, the superlayer, is Ni deposited with a high residual tension.
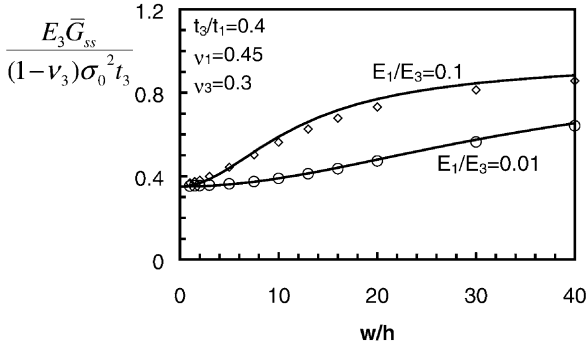
Fig. 12. Steady-state energy release rate for full delamination as a function of strip width. The open marks are from FEM calculations and solid curves are from Eq. (12).

5.1. Steady-state energy release rate

The steady-state energy release rate for both full delamination and partial delamination are calculated. For full delamination, the strain energy in the downstream slab can be assumed be negligible since the epoxy layer is much more compliant than the Ni superlayer $(E_1/E_3 \approx 10^{-3})$. The Ni layer is able to release almost all its stress since the epoxy layer, which is of comparable thickness, offers essentially no resistance. The strain energy in the upstream slab is the energy stored in the biaxially pre-stressed superlayer, which is reduced by the relaxation of the stress at the edges. The reduced problem for the upstream slab is a plane strain problem. Because the epoxy layer is so compliant compared to the superlayer, a one-dimensional shear lag model can be used to accurately describe the epoxy/superlayer combination [9]. The compliance of the epoxy layer enables one to derive relatively simple closed form approximations for the energy release rates of interest. In this approach, the shear strain γ in the epoxy is approximated by u/t_1 with $u(y)$ as the displacement of the Ni superlayer and t_1 as the epoxy thickness. Then, one can estimate the strain energy in the upstream slab and obtain the average steady energy release rate of a full delamination crack as (see the Appendix in Ref. [9] for analysis details)

$$\bar{G}_{ss} = \frac{(1-\nu_3)\sigma_0^2 t_3}{E_3}\left[1 - \frac{(1+\nu_3)l}{w}\tanh\left(\frac{w}{2l}\right)\right] \quad (12)$$

Here, $l = (E_3 t_1 t_3/(1-\nu_3^2)\mu_1)^{1/2}$ is proportional to the edge zone width, with $\mu_1 = E_1/[2(1+\nu_1)]$ as the shear modulus of the polymer and (t_1, t_3) as the thickness of the polymer layer and superlayer, respectively. In Eq. (12), $(1-\nu_3)\sigma_0^2 t_3/E_3$ is the limiting biaxial energy density of the Ni layer. If $w \approx l$, the pre-stress is relaxed across the entire width of the strip. Formula Eq. (12) is accurate when both the substrate and superlayer are much stiffer than the intermediate polymer layer. The

shear lag approximation becomes invalid when the strip is not wide compared to its thickness, and thus Eq. (12) does not give the correct limit for $w \approx t_1$. Fig. 12 presents a plot of $\bar{G}_{ss}$ as a function of strip width. The solid lines are calculated using Eq. (12) for $t_3/t_1 = 0.4$ with $E_1/E_3 = 0.01$ and 0.1. The characteristic length l in the two cases is $11.3t_1$ and $3.7t_1$, respectively. Note that the substrate modulus does not appear in Eq. (12). The dots represent results from finite element calculations in which the substrate has the same elastic properties as the superlayer. Additional finite element calculations reveal that the modulus of the substrate has a little effect on $\bar{G}_{ss}$ as long as the substrate modulus is many times that of the polymer.

Similarly, the steady-state energy release rate for partial debonding of a superlayer can also be estimated when the shear lag approximation is invoked giving

$$\bar{G}_{ss} = \frac{(1-\nu_3^2)\sigma_0^2 t_3}{E_3}$$
$$\times\left[\frac{1}{2} + \frac{l}{c}\tanh\left(\frac{w-c}{2l}\right) - \frac{l}{c}\tanh\left(\frac{w}{2l}\right)\right] \quad (13)$$

5.2. Convergent debonding for full delamination

When the interface crack approaches the end of the strip, $\bar{G}$ decreases to zero for the reasons discussed earlier. For an infinitely wide strip subject to plane strain constraint parallel to the crack front, a closed form expression for $\bar{G}$ can be derived [9] by applying the shear lag approach to the converging debond with the result:

$$\bar{G}(b) = \bar{G}_{ss}\tanh^2\left(\frac{b}{2l}\right) \quad (14)$$

Here, b is the remaining ligament and $\bar{G}_{ss} = \Lambda_0$ under the plane strain restriction. For full delamination of the unconstrained strip of finite width, Eq. (14) supplies a
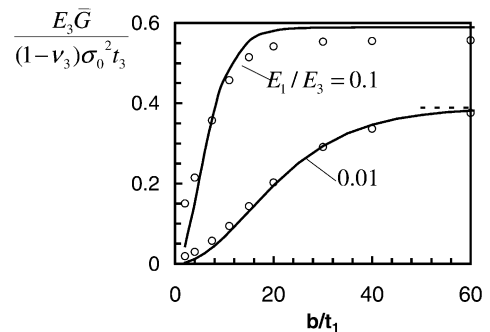

Fig. 13. Energy release rate for full delamination approaching the end of the super layer. The open marks are from FEM calculations and solid curves are from Eq. (14). The upper curve is for $E_1/E_3 = 0.1$ and the lower for $E_1/E_3 = 0.01$, both for $w/t_1 = 10$.

reasonable approximation if Eq. (12) is used for $\bar{G}_{ss}$ in formula Eq. (14). The energy release rate is plotted as a function of the remaining ligament, b, in Fig. 13 for $w/t_1 = 10$ and the same two values of E_1/E_3 used for the steady-state results in Fig. 12. The solid lines are based on Eq. (14) in conjunction with Eq. (12), and the discrete points are from finite element calculations. The Poisson ratios for the layers have been chosen as $\nu_1 = 0.45$, and $\nu_3 = 0.3$, and the ratio of the thickness or the layers is $t_3/t_1 = 0.4$. In Fig. 13, the energy release rate starts to deviate from the steady-state value when the remaining ligament is approximately $5l$.

Acknowledgments

References

[1] R.M. Cannon, R.M. Fisher, A.G. Evans, Mater. Res. Soc. Symp. Proc. 54 (1986) 799.
[2] A. Zhuk, A.G. Evans, G. Whitesides, J.W. Hutchinson, J. Mater. Res. 13 (1998) 3555.
[3] J.W. Hutchinson, Z. Suo, Adv. Appl. Mech. 29 (1992) 63.
[4] L.B. Freund, S. Suresh, Thin films and layered materials: stress, deformation and failure, Cambridge University Press, in press.
[5] H.H. Yu, J.W. Hutchinson, Int. J. Fract. 113 (2002) 39.
[6] A. Wikstrom, P. Gudmundson, S. Suresh, J. Appl. Phys. 86 (1999) 1113.
[7] ABAQUS, HKS Inc., Providence, RI, USA, 2001.
[8] H.H. Yu, M.Y. He, J.W. Hutchinson, Acta Mater. 49 (2001) 93.
[9] M.Y. He, A.G. Evans, J.W. Hutchinson, Acta Mater. 45 (1997) 3481.
[10] M.R. Begley, J.M. Ambrico, Int. J. Fract. 112 (2001) 205.
[11] G. Xu, M.Y. He, D.R. Clarke, Acta Mater. 47 (1999) 4131.
[12] A. Bagchi, G.E. Lucus, Z. Suo, A.G. Evans, J. Mater. Res. 9 (1994) 1734.